

Characterization and Thermal Decomposition Kinetics of Kapok (*Ceiba pentandra* L.)–Based Cellulose

Sarifah Fauziah Syed Draman,^a Rusli Daik,^{b*} Famiza Abdul Latif,^c and Said M. El-Sheikh^d

Interest in using kapok (*Ceiba pentandra* L.)–based cellulose in composite preparation is growing due to its advantages, including cost-effectiveness, light weight, non-toxicity, and biodegradability. In this study, chloroform, sodium chlorite, and sodium hydroxide were used for wax removal, delignification, and hemicellulose removal, respectively. It was observed that the air entrapment inside kapok fiber disappeared after it was treated with alkali. The structure became completely flattened and similar to a flat ribbon-like shape when examined using a vapour pressure scanning electron microscope (VPSEM). Fourier transform infrared (FTIR) spectroscopy was used to characterize the untreated and treated kapok fibers. The peak at 898 cm^{-1} , which is attributed to the glucose ring stretching in cellulose, was observed for the obtained cellulose samples. Peaks corresponding to lignin (1505 and 1597 cm^{-1}) and hemicellulose (1737 and 1248 cm^{-1}) disappeared. The results of differential scanning calorimetry (DSC) indicated that the degradation of cellulose appeared as an exothermic peak at about 300 to $350\text{ }^{\circ}\text{C}$. The activation energy for thermal decomposition of kapok cellulose and its hemicelluloses was 185 kJ/mol and 110 kJ/mol , respectively. The activation energy for thermal decomposition can be used as an alternative approach to determine the purity of cellulose.

Keywords: Biodegradable; Biomaterial; Renewable; Kapok cellulose

Contact information: a: Faculty of Applied Sciences, Universiti Teknologi MARA (Terengganu), 23000 Dungun, Terengganu, Malaysia; b: School of Chemical Sciences and Food Technology, Faculty of Science and Technology, Universiti Kebangsaan Malaysia, 43600 Bangi, Selangor, Malaysia; c: Faculty of Applied Sciences, Universiti Teknologi MARA (Malaysia), 40450 Shah Alam, Selangor, Malaysia; d: Nanostructured Materials and Nanotechnology Division, Central Metallurgical Research and Development Institute, 11421 Cairo, Egypt; *Corresponding author: rusli@ukm.my

INTRODUCTION

In recent years, many researchers have focused on development of smart materials with easy handling, lower cost, light weight, and biocompatibility. The interest in using cellulose in composite preparation has also increased. Cellulose has many advantages such as: abundant in nature, inexhaustible, low cost, easy processing, renewable, biodegradable, and biocompatible (Mahadeva *et al.* 2010).

A variety of lignocellulosic fibers have been studied including the pseudostem of the banana plant, sugarcane bagasse, sponge guard fibers (Guimarães *et al.* 2009), corn stalk, rice husk, sorghum straw, wheat straw (Varhegyi *et al.* 2011), coconut fiber (Rosa *et al.* 2010), and sesame husk (Bindu *et al.* 2011) for various applications. Generally cellulose is utilized as material for polymer composites in various applications such as a drug delivery system (Ge *et al.* 2010) as well as a flexible humidity and temperature

sensor (Mahadeva *et al.* 2010). Besides that, natural fibers can also be applied as a source for renewable energy (Panwar *et al.* 2011) and biofuels (Pirani and Hashaikeh 2012).

Kapok fiber has attracted increasing attention from many researchers. The fiber has been used for the enrichment culture of lignocelluloses-degrading bacteria (Nilsson and Björdal, 2008) and also as an oil absorbent (Abdullah *et al.* 2010; Rengasamy *et al.* 2011). Kapok fiber is obtained from the seed pods of the kapok tree (*Ceiba pentandra*) from the Bombacaceae family which originated in tropical India and is widespread in Southeast Asia (Rahmah and Abdullah 2011). The seeds are contained in capsules or pods that are picked and broken open with mallets. The fiber is exceedingly light with a circular cross-section, thin walls, and a wide lumen. Kapok fibers are moisture-resistant, buoyant, resilient, soft, and brittle. Traditional uses were in life jackets, sleeping bags, insulation, and upholstery. In Malaysia, kapok fiber is mainly used as a stuffing material for beds and pillows.

Cellulose is a relatively stable polymer. The cellulose fibers have good flexibility and elasticity compared with mineral fibers such as glass and carbon fibers. These properties allow them to maintain a high aspect ratio in the manufacturing process (Frone *et al.* 2011). The most interesting aspect about cellulose is its positive environmental impact. It is a renewable resource whose further production requires little energy. Carbon dioxide is used while oxygen is given back to the environment. The processing atmosphere is human-friendly with better working conditions, such that switching to such material generally will reduce dermal and respiratory irritation (John and Thomas 2008).

Obtaining pure cellulose from kapok fiber is essential due to its potential application as the matrix in polymer nanocomposite preparation. An epoxy group can be incorporated onto the cellulosic chain in order to introduce the adhesion capability that is important for applications such as coating materials in small electronic devices.

In this study, preparation and characterization were carried out to obtain pure cellulose from the kapok fibers. The contents of cellulose, hemicellulose, and lignin were usually determined by using wet chemical analytical methods (Rosli *et al.* 2013). These analytical procedures are standardized by American Society for Testing and Materials (ASTM) and the Technical Association of Pulp and Paper Industry (TAPPI) (Carrier *et al.* 2011). These wet chemical analytical methods are usually time-consuming and repetition is required for acceptable accuracy. Thus, thermal decomposition kinetic is employed in this study as an alternative approach to determine the purity of cellulose that requires minimum amount of sample as well as much less time.

Thermogravimetric analysis (TGA) is a widely used technique to study the decomposition of materials (Cabralés and Abidi, 2010). The thermal decomposition data generated can be analyzed and manipulated to obtain kinetic parameters such as activation energy. In order to calculate the activation energy, the most common "model-free" methods used are Friedman, Kissinger and Flynn-Wall-Ozawa (Muraleedharan and Kannan 2011; Sánchez-Jimenez *et al.* 2011). The advantage of using a "model-free" approach is that the calculation of activation energy can be carried out at different degrees of conversion without using any assumption specific to a particular reaction model. A thermal decomposition kinetics study was carried out in this study to find the activation energy of cellulose, hemicellulose, and lignin from kapok fiber as an alternative approach for determining the purity of cellulose. Such an approach has not been discussed by other researchers.

EXPERIMENTAL

Materials

Kapok fiber used in this study was obtained from Dungun, Terengganu, Malaysia. The fiber was isolated from the seeds and fruit cover. Visible dust and dirt were removed from the raw fiber.

Chloroform (CHCl_3) was purchased from R & M Chemicals, meanwhile sodium hydroxide (NaOH) and sodium chlorite (NaClO_2) were acquired from Friedemann Schmidt Chemicals and Sigma-Aldrich, respectively. Other chemicals were purchased from System. All chemicals were used as received.

Methods

Extraction of cellulose

Kapok fiber (4.0 g) was refluxed in CHCl_3 (400 mL, 4 h). The fibers were filtered, washed with methanol, and dried. CHCl_3 -treated fiber (8.0 g) was added to 800 mL distilled water and heated for 2 h at 70 to 80 °C. For the delignification process, dried CHCl_3 -treated fiber (3.0 g) was added to NaClO_2 (0.7 %, 300 mL) followed by acetic acid (2.0 mL). The mixture was heated for 3 h at 70 °C. After that, the fiber was filtered, and washed extensively with distilled water and methanol. The process was repeated three times. Then, NaClO_2 -treated fiber was dried at 40 °C in a vacuum until a constant weight achieved. Dried NaClO_2 -treated fiber (3.0 g) was then added to NaOH (4 %, 300 mL). The mixture was heated for 4 h at 85 °C. The obtained cellulose was later washed comprehensively with aqueous acetic acid and distilled water. Then, the fiber was dried in vacuum oven at 40 °C until a constant weight obtained.

Composition Determination of raw kapok fiber

Ash content was obtained from the decrease in weight when the dried fibers were subjected to calcination for 4 h at 800 °C. Lignin content was evaluated following the Technical Association of Pulp and Paper Industry (TAPPI) T13 wd-74 method. CHCl_3 -treated fibers (2.0 g) were macerated using 40 mL of 72% sulphuric acid (H_2SO_4) in a bath at about 2 °C. The acid was added gradually in small volumes with continuous stirring. The mixture was then kept at 20 °C for 2 h while stirring frequently to ensure a complete dissolution. Water (560 mL) was then added and the solution was refluxed for 4 h. The remaining solid was filtered and dried for 24 h at 40 °C. The lignin content was calculated by considering the weight difference between initial and final samples. The ash content was also subtracted from the final weight.

An amount of CHCl_3 -treated fiber (3.0 g) was added to NaClO_2 (5.0 g) in water (240 mL), followed by acetic acid (2.0 mL). The mixture was stirred for 3 h at 70 °C. After that, the fibers were filtered, washed extensively with distilled water and methanol, and later dried at 40 °C in a vacuum oven. This procedure was carried out to determine holocellulose content which is in accordance with TAPPI T 9 wd-75, indicating a selective degradation of the lignin.

Holocellulose (3.0 g) was added to NaOH (17.5%, 30 mL) at room temperature. The mixture was agitated for 8 min. Then, another 30 mL of 17.5% NaOH was added to the mixture and was kept at rest for 20 min at room temperature. The obtained fibers were later washed comprehensively with aqueous acetic acid and distilled water. Then, the fibers were dried in a vacuum oven at 40 °C. The amount of hemicellulose was

determined by deducting the α -cellulose content from the holocellulose. An average of three repetitions was employed for all mentioned analyses.

Characterization of kapok fiber

Infrared spectra of raw and treated kapok fibers were recorded using a PerkinElmer Fourier transform infrared (FTIR) spectroscope model GX. The powdered samples for each type of fiber were mixed with KBr and compressed into pellets. Samples were scanned from 400 to 4000 cm^{-1} . Thermogravimetric analysis (TGA) was carried out using a Mettler Toledo thermobalance (TGA/SDTA 851 $^{\circ}$). Samples of approximately 6 mg were placed in aluminum pans and heated from 30 $^{\circ}\text{C}$ to 800 $^{\circ}\text{C}$ at 10 $^{\circ}\text{C min}^{-1}$, under a dynamic flow of nitrogen (50 mL min^{-1}). Differential scanning calorimetric (DSC) analysis for the untreated and treated fibers was carried out using a Mettler Toledo DSC model 823 $^{\circ}$. Samples of approximately 6 mg were used. All samples were placed in aluminum sealed pans and heated from 30 $^{\circ}\text{C}$ to 600 $^{\circ}\text{C}$ at 10 $^{\circ}\text{C min}^{-1}$, under a dynamic flow of nitrogen (50 mL min^{-1}). Morphology of the fibers was examined by using a Zeiss vapor pressure scanning electron microscope (VPSEM), model Supra 55VP. The fiber samples were coated with gold using a Sputter Coater SC500 machine. SEM images were examined using an accelerating voltage of 15 kV.

Thermal decomposition kinetics

Thermal decomposition was studied by using a Mettler Toledo thermobalance (model TGA/SDTA 851 $^{\circ}$). Samples of approximately 6 mg were placed in aluminum pans and heated from 30 $^{\circ}\text{C}$ to 800 $^{\circ}\text{C}$ under a dynamic flow of nitrogen (50 mL min^{-1}). Five heating rates (5, 10, 15, 20, and 25 $^{\circ}\text{C min}^{-1}$) were used.

RESULTS AND DISCUSSION

Composition of Kapok Fibers

The color of Malaysian kapok fibers is pale yellowish brown, similar to the Philippine kapok. However, the color of Vietnamese kapok is pale yellow (Hori *et al.* 2000). Table 1 shows the chemical composition of kapok fibers used in this study as compared with reports by other researchers.

Table 1. Chemical Composition of Raw Kapok Fibers

Component (%)	Obtained	Reported	References
Ash	0.54 \pm 0.09	0.8 - Philippines kapok 0.5 - Vietnam kapok	Hori <i>et al.</i> 2000
Wax	5.31 \pm 0.29	About 3%	Choi and Moreau 1993, cited in Abdullah <i>et al.</i> 2010
Holocellulose	83.06 \pm 0.61	Not reported	
Lignin	20.73 \pm 0.21	13 21.5 - Philippines kapok 19.2 - Vietnam kapok	Reddy and Yang 2009 Hori <i>et al.</i> 2000
Cellulose	53.40 \pm 0.23	64 58.9 - Philippines kapok 62.9 - Vietnam kapok	Reddy and Yang 2009 Hori <i>et al.</i> 2000
Hemicellulose	29.63 \pm 0.62	Not reported	

It has been reported that the sum of all the chemical components in lignocellulosic material may not exactly equal 100% (Guimaraes *et al.* 2009). There are two reasons for this. First is the loss of polysaccharides during the isolation of cellulose by the reverse reaction during hydrolysis. The other reason is the overlapping of some of the components such as lignin residue in cellulose or ash.

Characterization of Kapok Fibers

FTIR spectroscopy

Figure 1 shows FTIR spectra of raw kapok and treated kapok fibers. Meanwhile, Table 2 summarizes major peaks of the spectra for raw and treated kapok fibers.

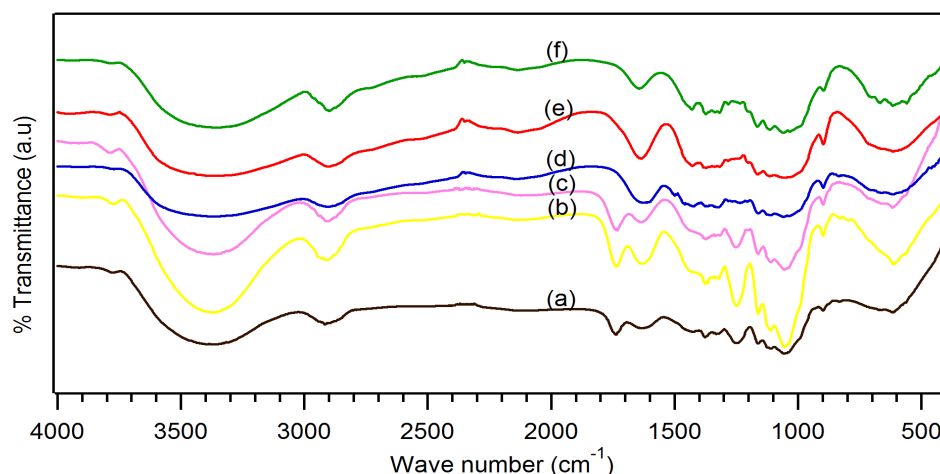


Fig. 1. FTIR spectra for (a) raw kapok fiber, (b) CHCl_3 -reated kapok fiber, (c) NaClO_2 -treated kapok fiber, (d) NaOH -treated kapok fiber, (e) obtained cellulose, (f) commercial MCC

Chloroform treatment was carried out to remove the kapok fibers' waxy surface. Increases in the intensity of bands at 1737 and 1248 cm^{-1} , which are correlated to the presence of the carbonyl group ($\text{C}=\text{O}$) of the ester bonds, were observed. These observations suggest the possibility of wax removal from the kapok fiber surface. These FTIR spectra were similar to those reported previously (Abdullah *et al.* 2010).

Lignin is an amorphous substance that is partly aromatic in nature. Lignin provides the structural rigidity, stiffening, and holding together of the fibers (Walia *et al.* 2009). Both peaks at 1504 and 1597 cm^{-1} are due to $\text{C}=\text{C}$ stretching and $\text{C}=\text{C}$ aromatic skeletal vibration of lignin, respectively (Bono *et al.* 2009). These two peaks were not observed in the FTIR spectra of the NaClO_2 -treated samples. However, the FTIR spectrum was quite similar to that of the CHCl_3 -treated samples. It seems that FTIR spectroscopy itself is not sufficient to describe the removal of lignin because most of lignin peaks are quite similar to those of hemicelluloses and cellulose (Rosa *et al.* 2010).

Alkali treatment with NaOH was carried out to remove hemicellulose. When the hemicelluloses are removed, the interfibrillar region is likely to be less dense and less rigid (Bledzki and Gassan 1999). In addition, NaOH is the most common chemical for cleaning the surface of the plant fibers (Mwaikambo and Ansell 2002). The use of NaOH with an appropriate concentration is essential to improve mechanical interlocking and the bonding reaction (Mwaikambo and Ansell 2002). Based on the results from FTIR spectroscopy, the removal of lignin and hemicelluloses was successful since peaks for lignin and hemicelluloses completely disappeared. Furthermore, the extracted kapok-

cellulose and commercial MCC exhibited identical FTIR spectra (Fig. 3e and 3f). Nazir *et al.* (2013) reported similar FTIR results for extracted OPEFB-cellulose and commercial MCC.

Table 2. Summary of the Main FTIR bands (cm^{-1})

Raw Kapok	CHCl_3 -treated Fiber	NaClO_2 -treated Fiber	NaOH -treated Fiber	Obtained Cellulose	Peak Assignment ^a	Description ^b
3358	3371	3364	3372	3205	O-H stretching	OH group
2918	2911				C-H stretching of aliphatic ($=\text{CH}_2$ and $-\text{CH}_3$)	
		2908	2904		C-H symmetric and asymmetric stretching	
				2894	C-H stretching	
		2370			Glucose ring stretching	Hemicellulose, cellulose, β -glucoside linkage
		2344				
2122	2129	2130	2127	2135	C-O-C stretching	β -glucoside linkage
1737	1738	1738	*	*	C=O stretching	Hemicellulose
1646	1643	1643	1644	1644.21	O-H deformation	H_2O
-	1598		1598		C=C stretching	Lignin
-	1506	*	1505	*	C=C aromatic skeletal vibration	Lignin
			1459		C=C aromatic skeletal vibration	Lignin
1424	1425	1427	1425	1430	C-H deformation	Cellulose and lignin
1374	1374	1376			C-H deformation	Cellulose, hemicellulose, and lignin
1333	1334		1332		O-H in plane deformation	Cellulose
		1320			CH_2 wag	Cellulose
1249	1249	1251	*	*	C-O stretching	Hemicellulose and lignin
			1235		C-O stretching	Acetyl group
1162	1162	1162	1161		C-O-C asymmetric stretching	Cellulose, hemicellulose and lignin
				1153	O-H stretching	Cellulose, lignin
1057	1051	1057	1060		C-O stretching	Hemicellulose, and lignin
900	899	899	898	898	Glucose ring stretching, C_1 -H deformation	Hemicellulose, cellulose, β -glucoside linkage
			665	669	C-OH bending	
614	613	614	616		C-OH bending	

^{a, b} based on discussion by Rosa *et al.* 2010, Guimarães *et al.* 2009, Rengasamy *et al.* 2011, Mwaikambo and Ansell 2002, Abdullah *et al.* 2010; * disappeared

According to Bono *et al.* (2009) and Sun *et al.* (2004), the peak observed at 898 cm^{-1} is attributed to the presence of β -glucoside linkage between glucose units in cellulose. This peak was found in all FTIR spectra in this study including the FTIR spectrum for the obtained cellulose fiber.

In the ^1H NMR spectrum of commercial MCC (spectrum not shown), the peaks at 4.69 and 4.27 ppm were assigned to the beta proton ($\beta\text{-H-1}_a$, $\beta\text{-H-1}$) of glucose (de la Motte *et al.* 2011). Meanwhile the peaks at 5.43 and 5.12 ppm were attributed to the alpha proton ($\alpha\text{-H-1}_a$, $\alpha\text{-H-1}$) of glucose (Huijbrechts *et al.* 2007). The broader peak between 3.50 and 2.95 ppm was assigned to the magnetically similar protons H-2 to H-5. The characteristics for the H-6 (2H) protons were identified at 3.88 and 3.79 ppm. The extracted cellulose also produced a similar ^1H NMR spectrum.

Morphology of kapok fiber

SEM micrographs for raw kapok fibers, treated kapok fibers, and obtained cellulose are shown in Fig. 2. A silky appearance and smooth surface can be seen for raw kapok fiber (Fig. 2a). Chloroform-treated kapok fibers (Fig. 2b) show that the silky appearance was reduced and some parts of the fibers were flattened. However, the buoyancy and fluffiness remained unchanged. The overall tubular structure was retained unbroken. This result was similar to a previous report by other researchers (Abdullah *et al.* 2010).

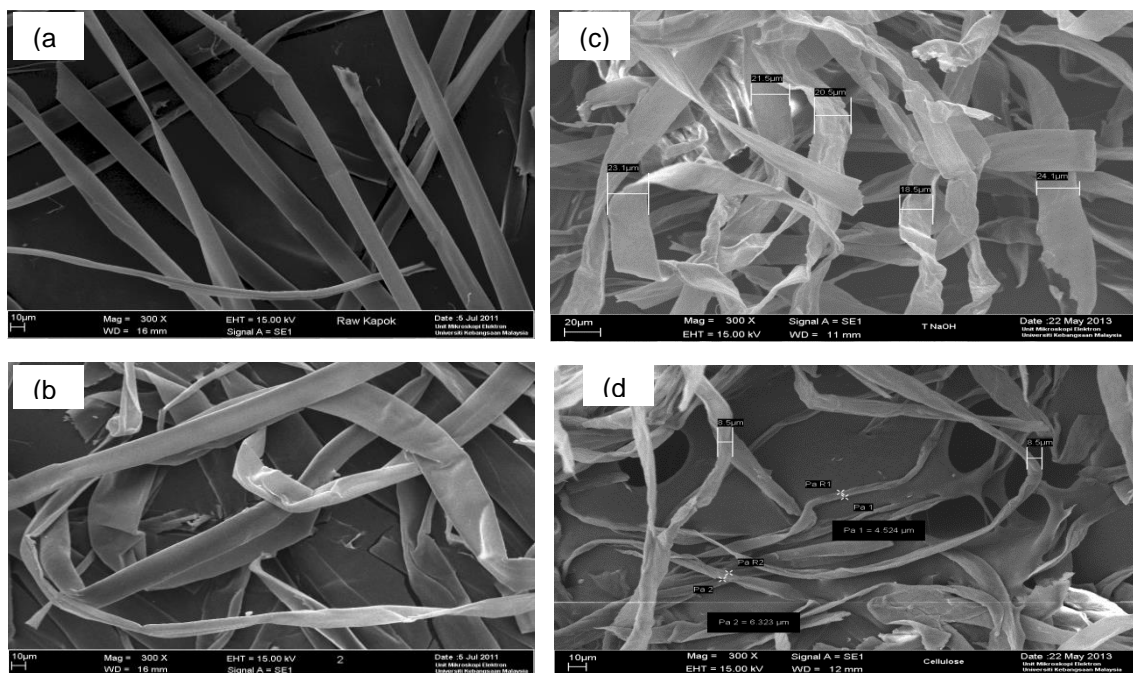


Fig. 2. SEM images of (a) raw kapok fibers, (b) CHCl_3 -treated fibers, (c) NaOH treated-fibers, and (d) obtained cellulose

The air entrapment inside the kapok fiber disappeared after alkali treatment (Fig. 2c). The structure became completely flattened with a flat ribbon-like shape. The surface of the kapok fibers was also rougher as compared with that of the untreated fibers. Alkali treatment was reported to increase the crystallinity due to the removal of non-cellulosic material (Bledzki and Gassan 1999). Figure 2d shows the SEM image of the obtained cellulose after chemical treatment with NaOH and NaClO_2 . The appearance was quite similar to that presented in Fig. 2c except that the length and diameter of fibers were reduced. After treatment with NaOH and NaClO_2 , the diameter range was 4.5 to 8.5 μm , whereas it was 18.5 to 23.1 μm for samples treated with only NaOH.

Thermal analysis of kapok fibers

Figure 3 presents the TGA thermograms and corresponding DTG curves of the raw and treated fibers. The obvious "shoulder" around 250 °C to 300 °C was normally ascribed to the thermal degradation for hemicelluloses in an inert atmosphere. The high-temperature "tails" around 400 °C to 600 °C were normally attributed to the degradation of lignin (Yao *et al.* 2008). For raw kapok (Fig. 3a), hemicelluloses' shoulder peaks were not obvious because they overlapped with the main peaks of cellulose. As shown in the thermogram of NaClO₂-treated fibers (Fig. 3b), the first peak appeared around 250 °C (shoulder), corresponding to the thermal degradation of hemicellulose (Alvarez and Vázquez 2004). It can be seen in the same DTG curve that no tail appeared around 400 °C to 600 °C, underlining the successful delignification process. The thermogram of NaOH treated-fiber (Fig. 3c) showed that there were no shoulders but tails were present above 350 °C. It can be stated that lignin remained in the fibers, since the treatment with NaOH only removed hemicellulose. For kapok fibers that went through both chemical treatments, there are no shoulders or tails present in the thermogram, indicating that lignin and hemicelluloses were successfully removed. The thermal degradation of cellulose at around 300 to 350 °C showed that cellulose fibers were successfully obtained (Fig. 3d).

In general, the thermolysis reactions of cellulose and hemicellulose occur by the cleavage of glycoside bonds, C-H, C-O, and C-C bonds. Dehydration, decarboxylation, and decarbonylation are also involved in the process (Trindade *et al.* 2005). One of the degradation mechanisms of lignin is considered to occur through dehydration, yielding derivatives with lateral unsaturated chains and the release of water. Carbon monoxide, carbon dioxide, and methane are also formed. The degradation of aromatic rings occurs above 400 °C. Continuous burning leads to the saturation of the aromatic rings, the rupture of C-C bonds present in lignin, the release of water, CO₂, and CO, and structural rearrangements. This description can be used to explain why lignin exhibits thermal degradation within a larger temperature range.

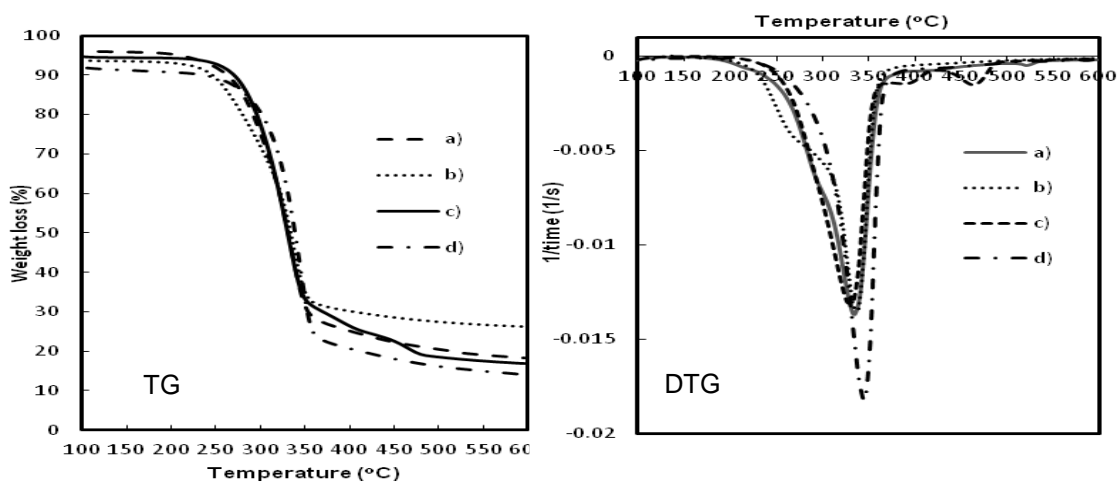


Fig. 3. TGA thermograms of (a) raw kapok fibers, (b) NaClO₂-treated fibers, (c) NaOH-treated fibers, and (d) obtained cellulose

DSC thermograms (Fig. 4) show peaks related to the degradation of untreated and treated fibers. The first exothermic peak appeared around 300 °C to 350 °C, indicating the degradation of cellulose. The second exothermic peak at 400 °C to 450 °C is likely to be due to oxidation of the char. The intensity of the second peak is higher and this might indicate self-ignition of the char (Soares *et al.* 1995). These DSC thermograms were similar to those reported by other researchers (Mwaikambo and Ansell 2002). It was observed that the chemical treatment could increase the thermal stability of materials. According to Moran *et al.* (2008), this is due to progressive removal of non-cellulosic material including hemicellulose and lignin. Johar *et al.* (2012) also reported similar observations in their research on rice husks. Both the obtained cellulose and MCC showed first exothermic peak at 330 °C.

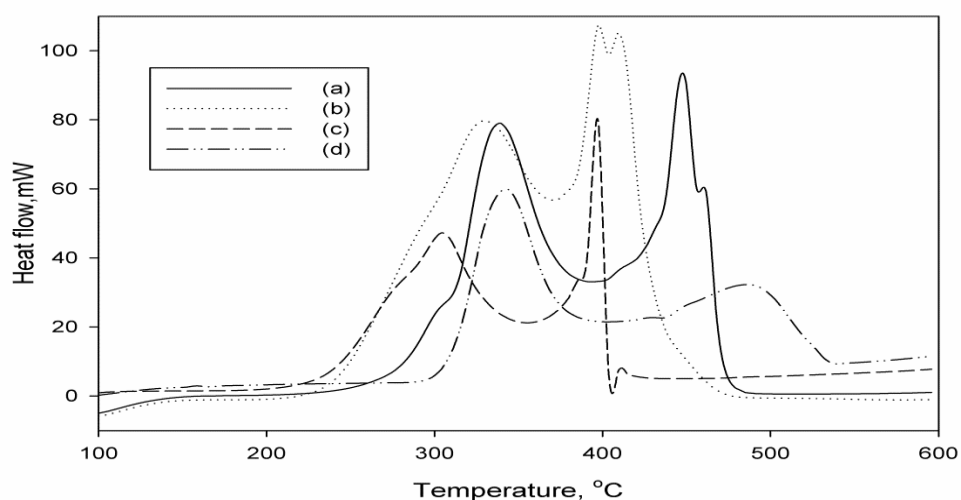


Fig. 4. DSC thermograms of (a) obtained cellulose, (b) NaOH-treated kapok fibers, (c) raw kapok fibers, and d) commercial MCC

Thermal Decomposition Kinetics

Thermogravimetric analysis (TGA) has been widely used for measuring thermal stability of various substances including polymers. This thermal analysis technique can quantify the changes rapidly (Alvarez and Vázquez 2004). The study of polymer degradation using TGA that involved derivation of kinetic data has also received great attention in the last decade regarding the determination of rate constants, activation energies, reaction orders, and Arrhenius pre-exponential constants. The values obtained depend upon atmospheric gas, sample mass, sample shape, flow rate, heating rate, and the mathematical treatment used to evaluate the data (Varhegyi *et al.* 2011).

The "model-free" iso-conversional methods are considered to be a helpful solution for accurately determining the activation energy (Yao *et al.* 2008). The approach allows obtaining the dependence of the kinetic parameters with the conversion from thermogravimetric (TG) and differential thermogravimetric (DTG) curves measured at different heating rates without making any assumption about the reaction function and reaction order. Therefore, the method can avoid any risk of obtaining the wrong kinetic parameters.

All kinetic studies are generally based on the basic rate equation as follows,

$$\frac{d\alpha}{dt} = k \cdot f(\alpha) \quad (1)$$

where k is the rate constant and $f(\alpha)$ is the reaction model, a function depending on the actual reaction mechanism. Equation (1) states that the rate of conversion, $d\alpha/dt$, at a constant temperature is a function of the reactant concentration loss and rate constant. The conversion rate α in this study is described as,

$$\alpha = \frac{(W_o - W_t)}{(W_o - W_f)} \quad (2)$$

where W_t , W_o , and W_f are weight at time(t), initial weight, and final weight of the sample, respectively.

The rate constant k is generally given by the Arrhenius equation,

$$k = A e^{-E_a/RT} \quad (3)$$

where E_a is the activation energy (kJ/mol), R is the gas constant (8.314 J/K mol), A is the pre-exponential factor (min^{-1}), and T is the temperature (K). The combination of Eqs. 1 and 3 gives the following relationship:

$$\frac{d\alpha}{dt} = A e^{-E_a/RT} f(\alpha) \quad (4)$$

For a dynamic TGA process, the heating rate is introduced, which is $\beta = dT/dt$, into Eq. 4, and therefore Eq. 5 is obtained.

$$\frac{d\alpha}{dt} = \left(\frac{A}{\beta}\right) \left(-\frac{E_a}{RT}\right) f(\alpha) \quad (5)$$

Equations (4) and (5) are the fundamental expressions of analytical methods used to calculate kinetic parameters based on TGA data.

Table 3 summarizes the most common "model-free" methods used in evaluating activation energy in this study (Kim *et al.* 2000; Yao *et al.* 2008).

Table 3. Three Kinetic Methods Used in This Study

Method	Expression	Plots
Friedman	$\ln\left(\frac{d\alpha}{dt}\right) = \ln[A f(\alpha)] - \frac{E_a}{RT}$	$\ln\left(\frac{d\alpha}{dt}\right)$ against $\frac{1}{T}$
Kissinger	$\ln\left(\frac{\beta}{T_p^2}\right) = \ln\left(\frac{AR}{E_a}\right) + \left(\frac{1}{T_p}\right) \left(-\frac{E_a}{R}\right)$	$\ln\left(\frac{\beta}{T_p^2}\right)$ against $\frac{1}{T_p}$
Flynn-Wall-Ozawa	$\log \beta = \log\left(\frac{AE_a}{Rg(\alpha)}\right) - 2.315 - 0.4567 \frac{E_a}{RT}$	$\log \beta$ against $\frac{1}{T}$

The Friedman method is the most general derivative technique. This iso-conversional method directly leads to $(-E_a/R)$ for a given value by plotting $\ln(d\alpha/dt)$ against $1/T$. In the Kissinger method, $\ln(\beta / T_p^2)$ is plotted against $1/T_p$ for a series of experiments at different heating rates with the peak temperature T_p . T_p was obtained from the DTG curve which is the temperature at which the maximum degradation (amount of

material) occurred. The iso-conversional Flynn-Wall-Ozawa (F-W-O) method is an integral method. The value of $-E_a/R$ is determined from the slope of the line by plotting $\log \beta$ against $1/T$ at any particular conversion rate.

Determination of activation energy from kapok fibers

Thermal degradation parameters were obtained from the TGA thermograms and corresponding DTG curves. Table 4 summarizes degradation characteristics of the fibers including peak at maximum degradation (T_p), weight loss, and residues detected from different heating rates. It was observed that the temperature at maximum degradation moved to higher values with increasing heating rate. Further increase in temperature led to an average residue of about 20%. There are two competitive pathways for thermal degradation, which are dehydration and depolymerization. Dehydration will produce char and gases, meanwhile depolymerization generates tar and gases. The high residues found in this study might be due to the production of char that retarded the unzipping reaction of depolymerization. Therefore, the dehydration pathway seems to be more favorable (Soares *et al.* 1995).

Figure 5 shows the plots of three model-free methods used in this study to determine the activation energy of kapok cellulose. It is shown in Fig. 5b and Fig. 5c that the fitted lines are nearly parallel. The general trend indicates that approximate activation energies at different conversions involved the possibility of a single reaction mechanism (or the unification of multiple reaction mechanisms) (Alvarez and Vázquez 2004). Meanwhile, Table 5 summarizes the activation energy calculated by the three methods for kapok cellulose.

Table 4. Degradation Characteristics of Cellulose and Hemicellulose of Kapok Fibers

Fiber	Heating Rate (°C/min)	T_p (°C)	Weight loss (%)	Residue (%)
Cellulose	5	332.0	80.26	18.58
	10	342.0	77.21	18.18
	15	350.0	73.56	27.07
	20	355.0	77.92	21.80
	25	358.0	77.04	23.28
				77.20 (2.41) ^a
Hemicellulose (NaClO ₂ - treated)	5	245.0	80.30	13.51
	10	255.0	78.23	21.02
	15	262.0	76.80	17.34
	20	265.0	75.67	23.16
	25	275.0	78.48	20.58
				77.90 (1.76) ^a

^a Values from five heating rates with mean value and standard deviation

It has been reported that typical activation energy for degradation of cellulose from wood is in the range of 195 to 213 kJ/mol (Gronli *et al.* 2002). In this study, the conversion rate between 0.6 and 0.8 gives results similar to previous reports. The average value for the activation energy of kapok cellulose obtained in this study was also similar to the activation energy for the degradation of starch and cellulose derivatives (182.3 kJ/mol) reported by Alvarez and Vázquez (2004).

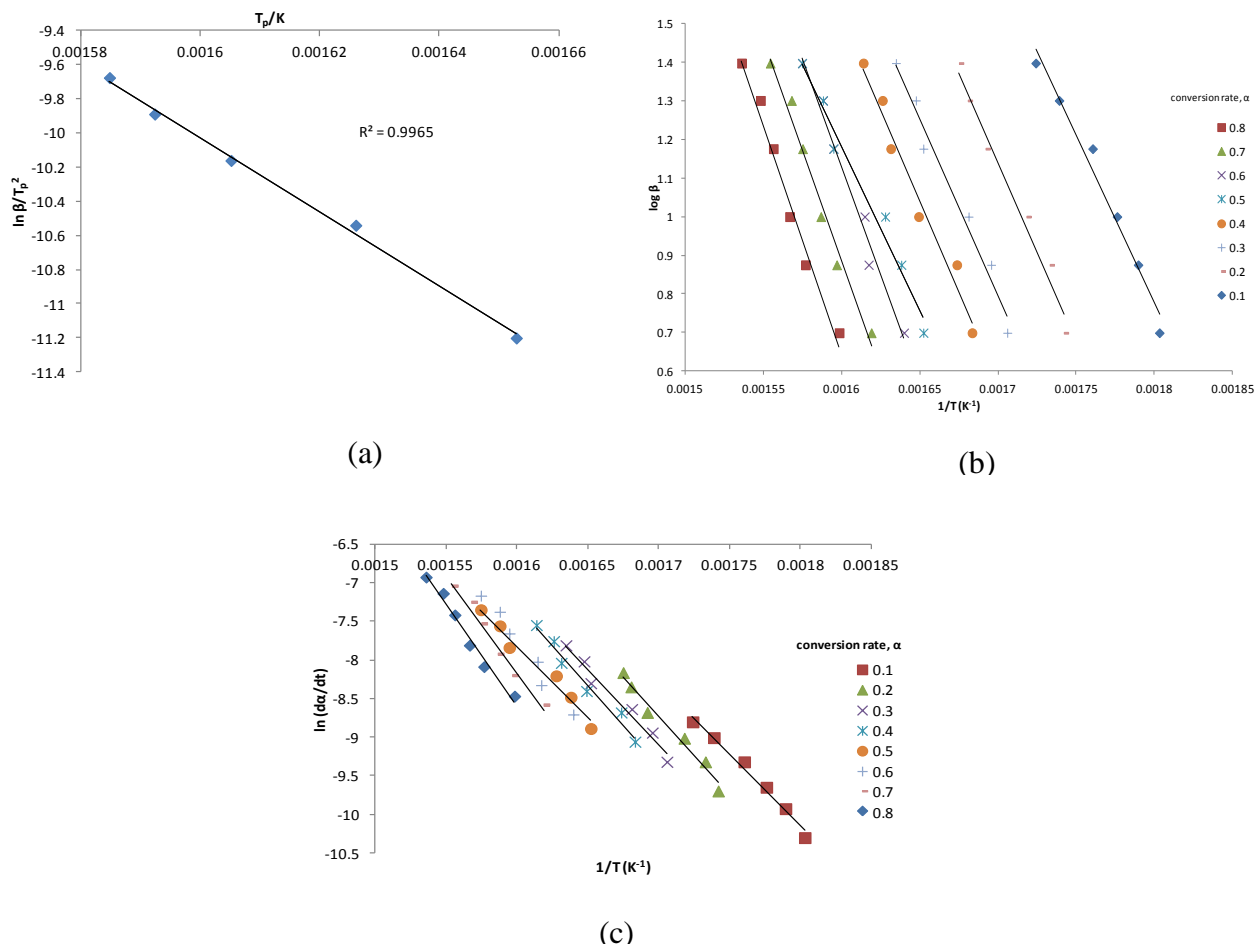


Fig. 5. Linear plots of kapok cellulose in (a) Kissinger, (b) Friedman, and (c) F-L-O methods

Table 5. Activation Energy for Degradation of Kapok Cellulose Determined by Kissinger, Friedman, and F-L-O Methods

Method	Conversion Rate, α	E_a (kJ/mol)	R^2
Kissinger		186.196	0.9965
Friedman	0.1	157.392	0.9841
	0.2	189.984	0.9752
	0.3	175.912	0.9716
	0.4	180.331	0.9729
	0.5	164.732	0.9739
	0.6	195.992	0.9765
	0.7	197.847	0.9785
	0.8	204.931	0.9796
		183.390 (16.753) ^a	0.9765(0.0041) ^a
F-L-O	0.1	160.640	0.9789
	0.2	189.945	0.9786
	0.3	178.403	0.9767
	0.4	186.633	0.9733
	0.5	163.807	0.9783
	0.6	194.887	0.9801
	0.7	196.575	0.9801
	0.8	203.460	0.9811
		184.294 (15.500) ^a	0.9784(0.0025) ^a

^a Values from eight conversion rates with mean value and standard deviation

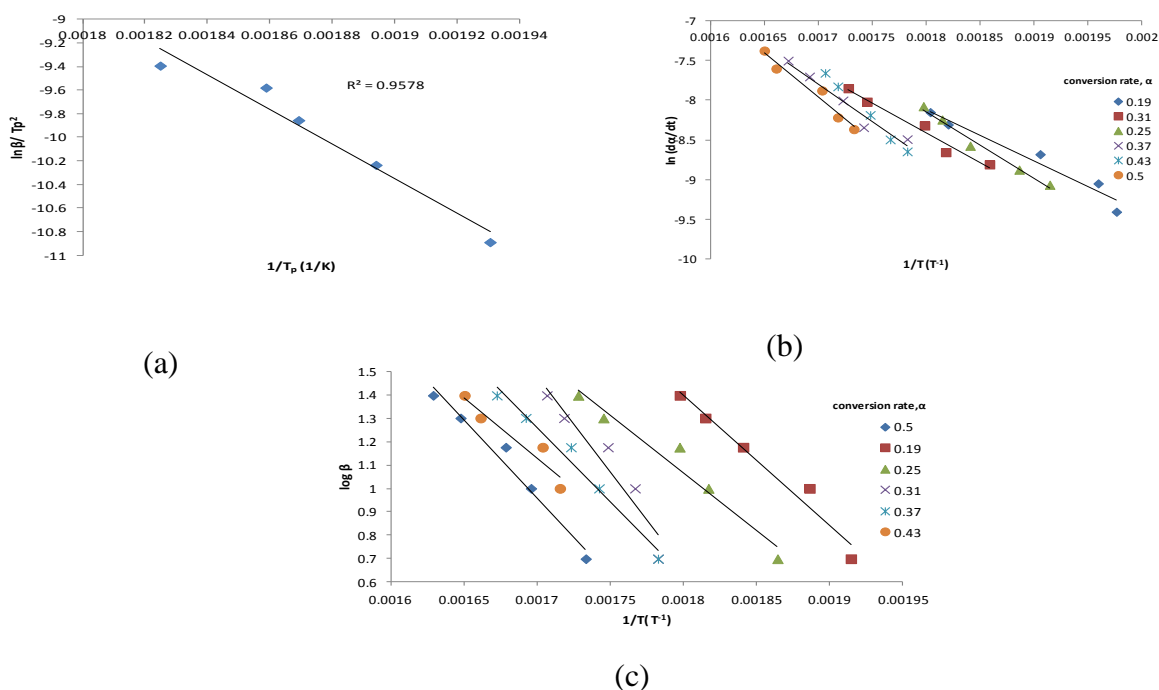


Fig. 6. Linear plots of kapok hemicellulose in (a) Kissinger, (b) Friedman, and (c) F-L-O methods

The degradation activation energy of Kapok hemicellulose was calculated according to the three model methods. In the Kissinger method, peak temperature (T_p) was determined from the shoulder peak of the DTG curves. The conversion rates for the Friedman and F-L-O methods were determined from 85% to 60% weight loss due to the degradation of hemicellulose near 300 °C (Trindade *et al.* 2005). Figure 6 and Table 6 show the plots of three model-free methods and the degradation activation energy of kapok hemicelluloses obtained in this study, respectively.

Table 6. Activation Energy for Degradation of Kapok Hemicellulose Determined by Kissinger, Friedman, and F-L-O Methods

Method	Conversion Rate, α	E_a (kJ/mol)	R^2
Kissinger		117.753	0.9578
Friedman	0.19	75.066	0.9540
	0.25	74.346	0.9687
	0.31	115.872	0.9963
	0.37	100.130	0.9561
	0.43	103.078	0.9625
	0.50	173.393	0.9631
		106.981(36.430) ^a	0.9668(0.0154) ^a
F-L-O	0.19	108.680	0.9936
	0.25	97.228	0.9543
	0.31	120.059	0.9717
	0.37	103.541	0.9686
	0.43	110.954	0.9605
	0.50	108.102	0.9623
		108.094(7.662) ^a	0.9685(0.0137) ^a

^a Values from eight conversion rates with mean value and standard deviation

Hemicellulose activation energies for wood degradation are between 105 and 111 kJ/mol (Yao *et al.* 2008). Alvarez and Vázquez (2004) also reported that the average activation energy for the first peak, which is considered for hemicellulose degradation, is 105.8 kJ/mol. In this study, average activation energy was similar to the results obtained by previous researchers (Yao *et al.* 2008; Alvarez and Vázquez 2004).

CONCLUSIONS

1. Cellulose was successfully extracted from kapok (*Ceiba pentandra* L.) using chemical treatments.
2. Results of the thermal degradation study using TGA showed that the activation energy of kapok cellulose and hemicelluloses was 184.627 kJ/mol and 110.943 kJ/mol, respectively. Both values are in the range of cellulose and hemicellulose that were reported for other fibers.
3. The activation energy values allow the development of a simple approach to better understand the thermal degradation behavior of natural fibers in relation to polymer nanocomposite processing in the future.
4. The activation energy can be used as an alternative parameter to determine the purity of cellulose fiber, especially kapok fiber.

ACKNOWLEDGEMENTS

The authors would like to acknowledge the Universiti Teknologi MARA and Ministry of Higher Education Malaysia for a scholarship. We would also like to express our gratitude to Universiti Kebangsaan Malaysia for providing the laboratory facilities, and for technical and financial support given throughout the research work.

REFERENCES CITED

- Abdullah, M. A., Rahmah, A. U., and Man, Z. (2010). "Physicochemical and sorption characteristics of Malaysian *Ceiba pentandra* L. Gaertn. as a natural oil sorbent," *J. Hazard. Mater.* 177, 683-691.
- Alvarez, V. A., and Vázquez, A. (2004). "Thermal degradation of cellulose derivatives/starch blends and sisal fibre biocomposites," *Polym. Degrad. Stab.* 84, 13-21.
- Bindu, S. P., Ray, D., Sengupta, S., Kar, T., Mohanty, A., and Manju, M. (2011). "Isolation of cellulose nanoparticles from sesame husk," *Ind. Eng. Chem. Res.* 50, 871-876.
- Bledzki, A. K., and Gassan, J. (1999). "Composites reinforced with cellulose based fibres," *Prog. Polym. Sci.* 24, 221-271.
- Bono, A., Ying, P. H., Yan, F. Y., Muei, C. L., Sratatly, R., and Krishniah, D. (2009). "Synthesis and characterization of carboxymethyl cellulose from palm kernel cake," *Adv. Nat. Appl. Sci.* 3(1), 5-11.

- Cabrales, L., and Abidi, N. (2010). "On the thermal degradation of cellulose in cotton fibres," *J. Therm. Anal. Calorim.* 102, 485-491.
- Carrier, M., Serani, A. L., Denux, D., Lasnier, J.-L., Pichavant, F. H., Cansell, F., and Aymonier, C. (2011). "Thermogravimetric analysis as a new method to determine the lignocellulosic composition of biomass," *Biomass Biotechnol.* 35, 298-307.
- de la Motte, H., Hasani, M., Brelid, H., and Westman, G. (2011). "Molecular characterization of hydrolyzed cationized nanocrystalline cellulose, cotton cellulose and softwood kraft pulp using high resolution 1D and 2D NMR," *Carbohydr. Polym.* 85, 738-746.
- Frone, A. N., Panaitescu, D. M., and Donescu, D. (2011). "Some aspects concerning the isolation of cellulose micro- and nano-fibers," *U.P.B. Sci. Bull. Series B* 73(2), 133-152.
- Ge, D., Ru, X., Hong, S., Jiang, S., Tu, J., Wang, J., Zhang, A., Ji, S., Linkov, V., Ren, B., and Shi, W. (2010). "Coating metals on cellulose-polypyrrole composites: A new route to self-powered drug delivery system," *Electrochem. Comm.* 12, 1367-1370.
- Gronli, M. G., Varhegyi, G., and Di Blasi, C. (2002). "Thermogravimetric analysis and devolatilization kinetics of wood," *Ind. Eng. Chem. Res.* 41, 4201-4208.
- Guimarães, J. L., Frollini, E., da Silva, C. G., Wypych, F., and Satyanarayana, K. G. (2009). "Characterization of banana, sugarcane bagasse and sponge gourd fibers of Brazil," *Ind. Crops Prod.* 30, 407-415.
- Hori, K., Flavier, M. E., Kuga, S., Tuyet Lam, T. B., and Iilama, K. (2000). "Excellent oil absorbent kapok [*Ceiba pentandra* (L.) Gaertn.] fiber: Fiber structure, chemical characteristics and application," *J. Wood Sci.* 46, 401-404.
- Huijbrechts, A. M. L., Huang, J., Schols, H. A., Van Lagen, B., Visser, G. M., Boeriu, C. G., and Sudhölter, E. J. R. (2007). "1-Allyloxy-2-hydroxypropyl-starch: Synthesis and characterization," *J. Polym. Sci. Part A : Polym. Chem.* 45, 2734-2744.
- Johar, N., Ahmad, I., and Dufresne, A. (2012). "Extraction, preparation and characterization of cellulose fibres and nanocrystals from rice husk," *Ind. Crops Prod.* 37, 93-99.
- John, M. J., and Thomas, S. (2008). "Biofibres and biocomposites," *Carbohydr. Polym.* 71, 343-364.
- Kim, W. I., Kim, S. D., Lee, S. B., and Hong, I. K. (2000). "Kinetic characterization of thermal degradation process for commercial rubbers," *J. Ind. Eng. Chem.* 6, 348-355.
- Mahadeva, S. K., Yun, S., and Kim, J. (2010). "Flexible humidity and temperature sensor based on cellulose-polypyrrole nanocomposite," *Sens. Actuator A: Phys.* 165(2), 194-199.
- Moran, J. I., Alvarez, V. A., Cyras, V. P., and Vázquez, A. (2008). "Extraction of cellulose and preparation of nanocellulose from sisal fibers," *Cellulose* 15, 149-159.
- Muraleedharan, K., and Kannan, M. P. (2011). "Thermal decomposition kinetics of potassium iodate," *J. Therm. Anal. Calorim.* 103, 943-955.
- Mwaikambo, L. Y., and Ansell, M. P. (2002). "Chemical modification of hemp, sisal, jute, and kapok fibers by alkalization," *J. Appl. Polym. Sci.* 84, 2222-2234.
- Nazir, M. S., Wahjoedi, B. A., Yussof, A. W., and Abdullah, M. A. (2013). "Eco-friendly extraction and characterization of cellulose from oil palm empty fruit bunches," *BioResources* 8(2), 2161-2172.
- Nilsson, T., and Björdal, C. (2008). "The use of kapok fibres for enrichment cultures of lignocellulose-degrading bacteria," *Inter. Biodeter. Biodeg.* 61, 11-16.

- Panwar, N. L., Kaushik, S. C., and Kothari, S. (2011). "Role of renewable energy sources in environmental protection: A review," *Renew. Sustain. Energy Rev.* 15, 1513-1524.
- Pirani, S., and Hashaikh, R. (2012). "Nanocrystalline cellulose extraction process and utilization of the byproduct for biofuels production," *Carbohydrate Polymers* 93(1), 357-363.
- Rahmah, A. U., and Abdullah, M. A. (2011). "Evaluation of Malaysian *Ceiba Pentandra* L. Gaertn. for oily water filtration using factorial design," *Desalination* 266, 51-55.
- Reddy, N., and Yang, Y. (2009). "Properties and the potential applications of natural cellulose fibers from the bark of cotton stalks," *Bioresour. Technol.* 100, 3563-3569.
- Rengasamy, R. S., Das, D., and Karan, C. P. (2011). "Study of oil sorption behavior of filled and structured fiber assemblies made from polypropylene, kapok and milkweed fibers," *J. Hazard. Mater.* 186, 526-532.
- Rosa, M. F., Medeiros, E. S., Malmonge, J. A., Gregorski, K. S., Wood, D. F., Mattoso, L. H. C., Glenn, G., Orts, W. J., and Imam, S. H. (2010). "Cellulose nanowhiskers from coconut husk fibers: Effect of preparation conditions on their thermal and morphological behavior," *Carbohydr. Polym.* 81, 83-92.
- Rosli, N.A, Ahmad, I, and Abdullah, A. (2013), "Isolation and characterization of cellulose nanocrystals from *Agave angustifolia* fibre," *BioResources* 8(2), 1893-1908.
- Sánchez-Jimenez, P. E., Perez-Maqueda, L. A., Perejon, A., Pascual-Cosp, J., Benitez-Guerrero, M., and Criado, J. M. (2011). "An improved model for the kinetic description of the thermal degradation of cellulose," *Cellulose* 18: 1487-1498.
- Soares, S., Camino, G., and Levchik, S. (1995). "Comparative study of the thermal decomposition of pure cellulose and pulp papers," *Polym. Degrad. Stab.* 49, 275-283.
- Sun, J. X., Sun, X. F., Zhao, H., and Sun, R. C. (2004). "Isolation and characterization of cellulose from sugarcane baggase," *Polym. Degrad. Stab.* 84, 331-339.
- Trindade, W. G., Hoareau, W., Megiatto, J. D., Razera, A. T., Castellan, A., and Frollini, E. (2005). "Thermoset phenolic matrices reinforced with unmodified and surface-grafted furfuryl alcohol sugar cane bagasse and curaua fibers: Properties of fibers and composites," *Biomacromol.* 6, 2485-2496.
- Varhegyi, G., Bobaly, B., Jakab, E., and Chen, H. (2011). "Thermogravimetric study of biomass pyrolysis kinetics. A distributed activation energy model with prediction tests," *Energy Fuels* 25, 24-32.
- Walia, Y. K., Kishore, K., Vasu, D., and Gupta, D. K. (2009). "Physico-chemical analysis of *Ceiba pentandra* (Kapok)," *Inter. J. Theor. Appl. Sci.* 1(2), 15-18.
- Yao, F., Wu, Q., Lei, Y., Guo, W., and Xu, Y. (2008). "Thermal decomposition kinetics of natural fibers: Activation energy with dynamic thermogravimetric analysis," *Polym. Degrad. Stab.* 93, 90-98.

Article submitted: March 11, 2013; Peer review completed: April 29, 2013; Revised version received: October 27, 2013; Accepted: October 28, 2013; Published: November 4, 2013.